A Study of Sensitivity of WRF Simulation to Microphysics Parameterizations, Slope Option and Analysis Nudging in Haean Basin, South Korea

Kim, Jea-Chul (1); Lee, Chong Bum (1); Belorid, Miloslav (1); Zhao, Peng (2)

(1) Department of Environmental Science, Kangwon National University, Chuncheon, South Korea, kjc25@kangwon.ac.kr
(2) Department of Micrometeorology, University of Bayreuth, 95440 Bayreuth, Germany, peng.zhao@uni-bayreuth.de

Abstract: An accurate representation of meteorological processes is important for improvement of meteorological predictions. In this study, the Weather Research and Forecasting model (WRF) is utilized to examine the sensitivity of meteorological simulations using two microphysics schemes and analysis nudging in the framework of the Complex TERRain and ECOlogical Heterogeneity (TERRECO) project. Model results for the most significant meteorological variables were assessed through a series of common statistics. In this study we compared several model configurations. The results of the *Lin et al.* schemes show good agreement with observations compared to those of the WSM6 schemes in rice paddy fields. Especially, RMSE of temperature and wind speed improved with *Lin et al* at rice paddy fields. However, the statistical results in mountain slopes showed worse results compared to other observation sites. Simulated temperature in KR-R is significantly overestimated during nights but in good agreement during day time when FDDA is used. This refers to both FDDA W and FDDA L cases.

Key words: *WRF, sensitivity, microphysics schemes, Haean Basin*

1. Introduction

As we have observed from past air pollution events, atmospheric phenomena in basins are important for dispersion and advection of pollutants (Rutllant and Garreaud, 1994; Whiteman et al., 2004).

The accuracy of numerical weather prediction (NWP) depends on the quality of the forecast model and initial conditions. It is well known that land-surface processes play an important role in exchanges of heat, moisture, and momentum between the surface and atmosphere. And it is important to represent them realistically in NWP. Several land-surface models with various complexities in physical processes have already been coupled to not only general circulation models but also regional and mesoscale models. In addition, initialization methods of producing land-surface states reflecting the real world are under development (e.g., Lu et al., 2005). In the modeling framework, it depends on both the performance of land surface model (LSM) and the accuracy of land surface initial conditions (Kim, 2010).

The meteorological model selected to provide the meteorological fields required by the dispersion and advection modeling is the Weather Research and Forecasting (WRF) modelling system. This non-hydrostatic mesoscale model system is based on the Fifth-Generation Penn State/NCAR Mesoscale Model (MM5) (Grell et al., 1994). The WRF is a next generation, fully compressible, Euler non-hydrostatic mesoscale forecast model with a run-time hydrostatic option. This model is useful for downscaling of weather and climate ranging from a kilometer to thousands of kilometers and useful for deriving meteorological parameters required for air quality models. The model uses a terrain-following hydrostatic pressure coordinate system with permitted vertical grid stretching (Laprise, 1992). Arakawa-C grid staggering is used for horizontal discretization.

This study focuses on particular schemes, input datasets and specific physical options implemented in WRF for applications over limited geographical areas of complex terrain. However, there is still lack of comprehensive sensitivity analysis of the WRF over the complex terrain. Therefore, we understand the Haean basin as a challenge and opportunity for WRF sensitivity testing. An additional objective of this research was to improve resolution of topography and use to improve the accuracy of theWRF model and to make a comparison with commonly available input data from sources such as the USGS. The specific objectives of the research are to determine the consequences of these processes on thermal flux transport and diffusion in the basin, and to

determine how meteorological models can be improved to provide more accurate simulations of persistent inversions.

2. Methodology

2.1 Modeling Domains and Initialization

The mother domain (D1) with 27 km spatial resolution, centered at 38°N, 126°E covers the Korean Peninsula, Japan, and East China (Figure 1). The innermost domain (D5) is centered over the Haean basin and consists of 54 columns and 57 rows of 0.3 X 0.3 km^2 grid cells. The five domains interact with each other through a two-way nesting strategy. The vertical structure of the model includes 36 layers. Topography and land use datasets were interpolated from the ASTER Global Digital Elevation Model (ASTER GDEM) and Korea Ministry of Environment (KME) with the appropriate spatial resolution for each domain (30' and 3' for D1, D2, D3, D4 and D5 respectively). The KME medium-category land use classification was considered to represent dominant vegetation types. The WRF simulations were driven by the National Centers for Environmental Prediction (NCEP) Global Data Assimilation System (GDAS) with 1° X 1° spatial resolution and temporal resolution of 6 h. The initial meteorological condition was determined using the regional data assimilation and prediction system (RDAPS), which was provided by Korea Meteorological Administration (KMA) with 30km spatial and temporal resolution of 3h.
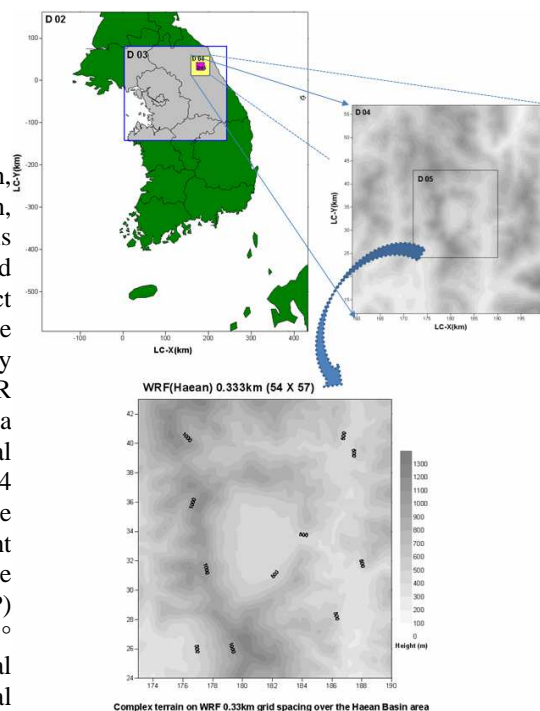
Figure 1. Domain architecture for WRF used for this application. Grid sizes for domain 2, 3, 4 and 5 are 9km, 3km, 1km, 0.33km, respectively.

2.2 Observation and Observed Flux Determination

The land use type for KR-R are rice paddies with a terrain slope of ca. 3°. Haean is an intensively used landscape located at longitude 128° 5' to 128° 11' E, latitude 38° 13' to 38° 20' N, with an altitude ranging from ca. 500 m (valley) to 1100 m (mountain ridge). The average annual air temperature in 2010 is ca.10.5°C at the valley sites and ca. 7.5°C at the mountain ridge. Average precipitation is estimated at 1200 mm with 50% falling during the summer monsoon season. Rice paddies and potato fields are two major types of farmlands in Haean, covering ca. 25% and 15% of the farmland area, respectively. More details about KR-P and KR-R can be found in Zhao et al. (2011).

For a comparison with the WRF simulation results, three observation site were selected (Figure 2). The observation sites are irrigated farmland for flux measurements (KR-R, 38°17' N, 128°08' E, 457m a.s.l), AWS-1 (A1,38°19' N, 128°07' E, 1049m a.s.l) at the mountain crest and AWS-10 (A10, 38°16'

Figure 2. The research sites in Haean Basin, South Korea.

N, 128°06' E, 630m a.s.l) on the west slope. The observations at KR-P and KR-R were carried out during a field campaign (June 1 to November 6, 2010) of the TERRECO project. Meteorological sensors were used for the measurement of air temperature, pressure, wind speed, and global radiation. Eddy covariance method was used to obtain the turbulent fluxes of sensible and latent heat from the measurement of an ultrasonic anemometer and a fast-response H_2O/CO_2 analyzer at a frequency of 20 Hz. In this study, the model results were compared only KR-R between two flux measurement stations. We used the software package TK2 (Mauder and Foken, 2004) to calculate and correct turbulent fluxes of sensible heat and latent heat from raw high frequency data. The correction strategy includes spike check (Vickers and Mahrt, 1997), planar fit (Wilczak et al., 2005), spectral corrections (Moor, 1986), conversion from sonic temperature fluctuations to real temperature fluctuations

(Schotanus et al., 1983), density correction for water vapour (Webb et al., 1980), interative determination, and quality control (Foken and Wichura, 1996; Foken et al., 2004). Selected fluxes have a good quality with quality flags of 1 to 6.

2.3 Episode Selection

Simulations were conducted during one period of the month; from 23 September 00h UTC to 28 September 00h UTC. The wind was relatively weak and a large temperature difference occurred between day and night during the episode period. Additionally, fog was observed in the morning and evening. As observed in the weather synopsis pattern (Figure 3), the entire Korean Peninsula was impacted by the high pressure condition. Also during the episode period, the *Typhoon* Malakas changed course from the sea south of Japan to north-east of Japan.
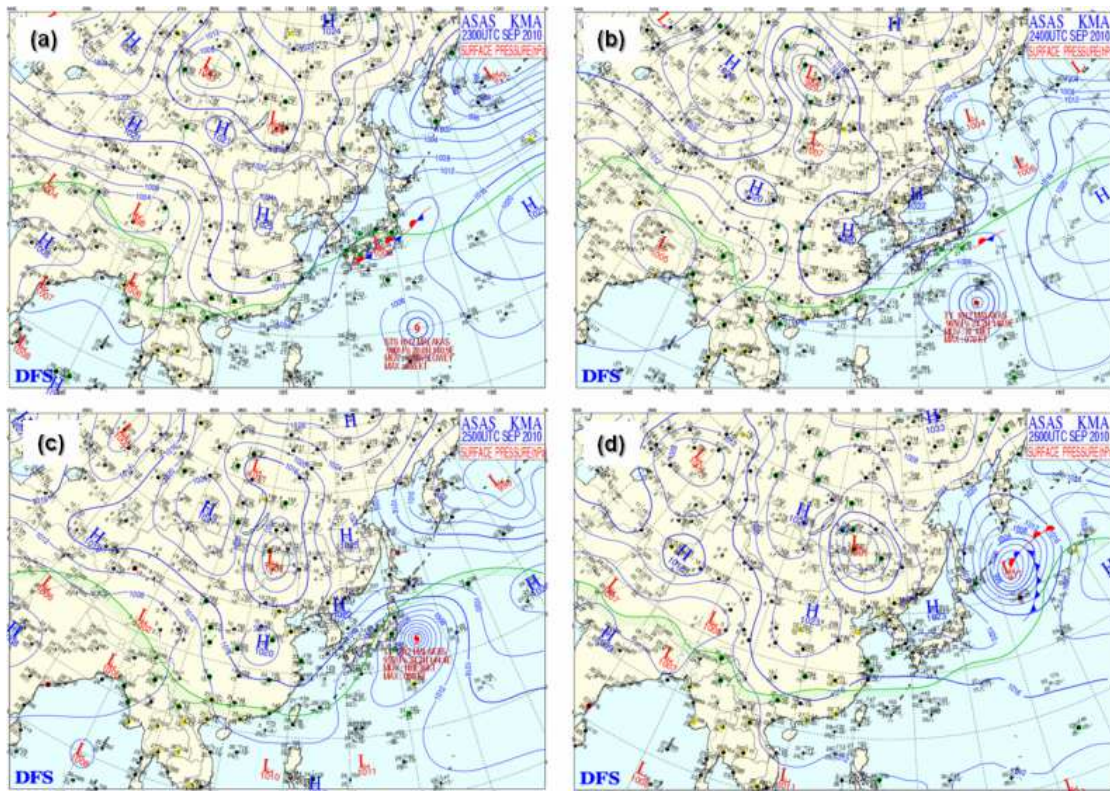
Figure 3. Synoptic surface weather map at (a) 0900 LST on September24, (b) 0900 LST on September 25, (c) 0900 LST on September 26, (d) 0900 LST on September 27, 2010.

2.4 Setting of the Sensitivity Analysis

We analyzed the sensitivity of the model by varying microphysics and radiation slope options with a proven physical option (Borge R. et al., 2008; Akylas, E. et al., 2007; Hong and Lim, 2006) for complex terrain of basin area based on previous study. The microphysics and slope option combinations are shown in Table 1. For the CASE A simulation physics options in this study, the Yonsei University (YSU) planet boundary layer scheme (Hong et al., 2006) was adopted. The YSU scheme is a modification of the MRF (medium-range forecast) scheme to include explicit entrainment fluxes of heat, moisture and momentum, counter-gradient transport of momentum, and different specifications of the PBLH. RRTM radiation scheme, WSM 6-class microphysics (Hong and Lim, 2006) and the Noah land surface model were used over the simulation period.

Table 1. Sensitivity test configuration combinations used in WRF simulations. Fdda W and Fdda L are WSM6 with FDDA, Lin et al with FDDA, respectively.

	Microphysics		Slope option	
	WSM6	Lin et al.	Yes	No
Case A	O			O
Case B	O		O	
Case C		O		O
Case D		O	O	
Analysis nudging				
Fdda W	O		O	
Fdda L		O	O	

Since the grid size is very fine, no cumulus scheme was used. A study of WRF thick coastal fog simulations by Ajjaji et al. (2008) shows that among all microphysics schemes the most realistic is the Lin scheme (Lin et al. 1983; Chen and Sun 2002). During our simulation periods, a radiation fog appeared in Haean Basin almost every night. Therefore we utilized the Lin scheme in our simulation as well and compared with WSM6. The RRTM longwave and Dudiah shortwave radiation schemes were used. The Dudiah shortwave scheme provides slope and shadow options. Finally, we used KME data as input and performed analysis nudging.

3. Results

3.1 Input Data Modified

Figure 4 shows the results of the different topography data used as WRF model input data (USGS, SRTM and ASTER_GDEM). Both USGS and SRTM show significant differences of mountain slope and mountain ridge elevation. Kim (2010) reported that improved resolution affected the WRF model results for complex terrain and fine grid areas. Jeong and Kim (2009) indicated that the improvement of land cover caused a temperature change on wide areas of inland and a nearby sea region, and narrow areas along the coastal line. Figure 5 shows difference of land use in Haean. We found that the USGS land use data is unrealistic for the Haean Basin. More realistic land use data are provided by KME with 3'' resolution. However, while the KME data is accurate for urban areas, it is insufficient for rural regions. We found some significant differences in land use between the TERRECO and KME data. The TERRECO data is more exact especially in case of rice paddy fields than KME for the Haean basin. Therefore, in this study only ASTER_GDEM topography data and TERRECO land use data were used as input data to the WRF model for the model sensitivity study.
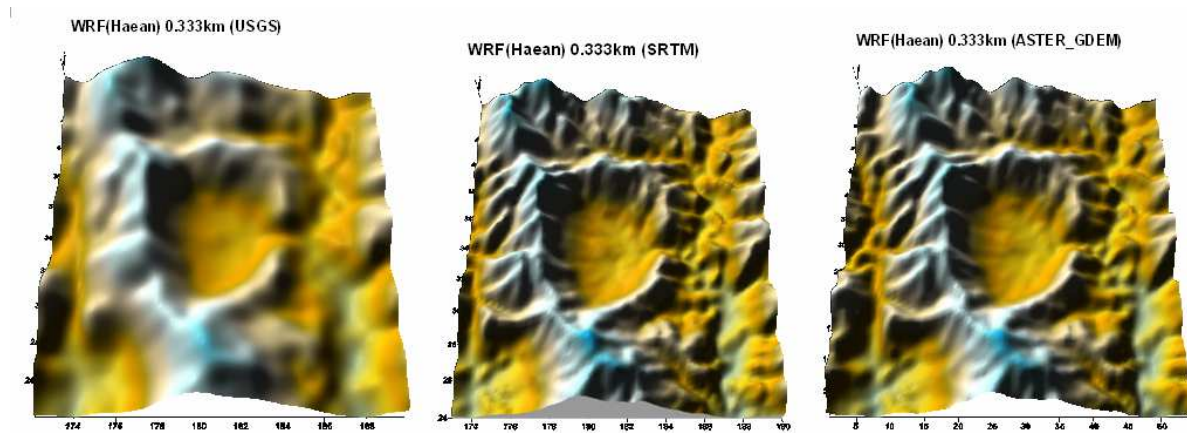
Figure 4. Comparison of topography difference with spatial resolution in Haean basin. Spatial resolutions for USGS, SRTM and ASTER_GDEM are 30", 3", 1", respectively.
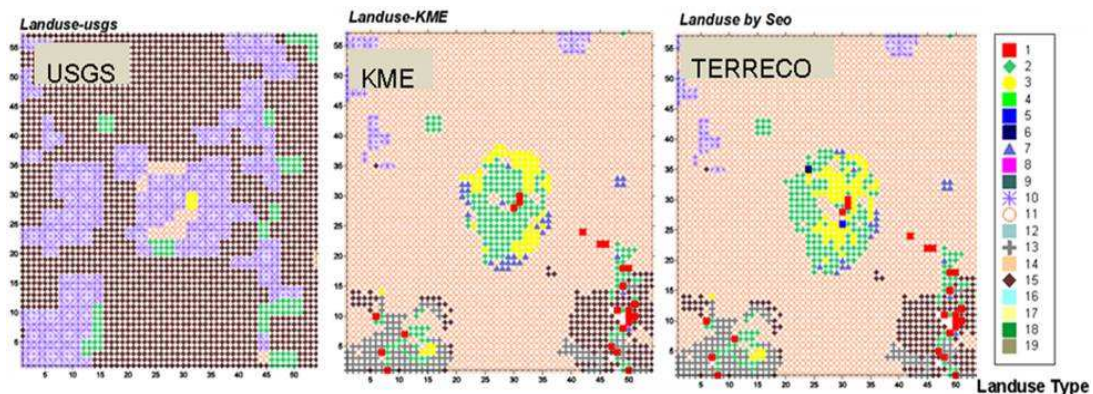
Figure 5. The land-use derived from the output of WPS preprocess for three case USGS, KME and TERRECO on D05 in Korea

3.2 Results of the Sensitivity Analysis

Statistical variables are used to evaluate the performance of the model via comparing the model-simulated data (Cp) and the observed data (Co). Brief definitions are given below (Table 2). More details can be found in study of Willmott (1982), Hanna (1994), Olerud and Wheeler (1997), Song (2007). The root-mean-square error

(RMSE) is a frequently used to measure of the differences between values predicted by a model and the values actually observed from the thing being modeled or estimated. Bias is systematic favoritism present in data collection, analysis or reporting of observations and simulation results.

The *Lin et al* scheme was found to produce good performance for temperature at the A10 and KR-R sites, as shown in Table 3. Site A1 at mountain crest was underestimated in the overall sensitivity configuration. Results for the two nudging strategies tested show no significant difference between Fdda W and Fdda L. In contrast, the RMSE of Fdda W seems to be equal or less than Fdda L for the mountain crest site as well as the basin bottom. However, the WSM 6 scheme was found to produce good performance for solar radiation at the A1 and A10 sites. It can be observed that all cases provide a similar *r* value of solar radiation for KR-R. The microphysics options were found to have no significant influence for the solar radiation simulations.

Overall, the WRF model results are mostly underestimated compared to observed values. In the case of wind speed, the RMSE is minimized for most of the stations, especially at the KR-R site where the lowest value was observed (0.6 m/s, Table 3). Also, CASE A showed the highest correlation coefficient value A1 and KR-R, 0.91 and 0.78, respectively. The slope and shadow options had little or no effect. More study is needed regarding the sensitivity of slope and shadow in complex terrain.

In the FDDA cases, the calculated temperature, solar radiation and wind speed based on microphysics schemes were underestimated.

Figure 6 shows a time series of observed and simulated temperature, wind speed, sensible heat flux and latent heat flux at the KR-R site. Simulated temperature is significantly overestimated during the nights but good agreement during the day time was observed when FDDA was used. This refers to both Fdda W and Fdda L cases. Wind speed is overestimated by CASE A. Other CASES are in relatively good agreement with observed values. An unexpected result was in a CASE C for the Lin scheme. The latent heat is markedly overestimated.

Table 2. The statistical treatment methods for the comparison of data (Song, 2007)

Item	Equation
Correlation coefficient (r)	$r = \dfrac{\sum\limits_{j=1}^{m}\sum\limits_{i=1}^{n} y_{o,i,j} y_{p,i,j}}{\sqrt{\sum\limits_{j=1}^{m}\sum\limits_{i=1}^{n} y_{o,i,j}^2 \sum\limits_{j=1}^{m}\sum\limits_{i=1}^{n} y_{p,i,j}^2}}$
Root Mean Square Error (RMSE)	$RMSE = \sqrt{\dfrac{1}{n}\sum\limits_{i=1}^{n}(C_{p,i} - C_{o,i})^2}$
Mean Bias (MB)	$MB = \dfrac{1}{N}\sum\limits_{i=1}^{N}(C_{p,i} - C_{o,i})$
Fractional Bias (FB)	$FB = \dfrac{\overline{C_p} - \overline{C_o}}{0.5(\overline{C_p} + \overline{C_o})}$

C_p: predicted concentration, C_o: observed
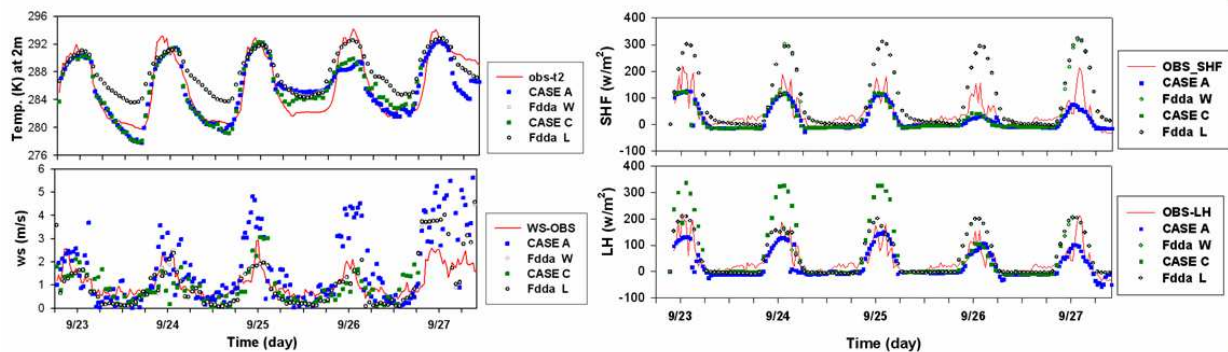
Figure 6. Time series of observed and simulated temperature at a height of 2 m, wind speed, sensible heat flux and latent heat flux at KR-R site in Haean Basin

4. Discussion and Conclusions

This study examines the sensitivity of meteorological simulations from WRF to Microphysics processes, slope and shadow option applications, and analysis nudging methods for a 5-day autumn episode in the Haean basin. First of all, ASTER_GDEM topography data and TERRECO land use data were used as input data for the WRF model for the model sensitivity study. Meteorological simulations show small to significant sensitivity to Microphysics schemes. The two PBL schemes, WSM6 and Lin et al, give overall similar simulations for T2, WS10, and SR. The results of the *Lin et al* schemes show good agreement with observed values as compared to those of the WSM6 schemes in KR-R. Especially, the RMSE of temperature and wind speed improved with *Lin et al* at KR-R. However, the statistical results at the mountain slope showed lower results when compared to the

observation site. Despite consideration of slope and shadow options, the WRF model results did not indicate a significant effect.

The results from this study indicate a need to refine model treatments at a high resolution input data and the analysis nudging method including slope options used in the WRF model for improvement of model performance. More studies of the complex terrain must be completed before it is ready for generalization.

Table 3. Analysis of statistics between WRF model results and observation sites with altitude. A1, A10 and KR-R are the observatory site, western forest site, rice field site, respectively.

Temperature (K)

Statistic	CASE	A1	A10	KR-R
R	CASE A	**0.83**	0.76	0.84
	CASE B	0.77	0.72	0.84
	CASE C	0.72	0.82	**0.89**
	CASE D	0.73	0.81	**0.89**
	Fdda W	0.80	**0.85**	**0.89**
	Fdda L	0.80	**0.85**	**0.89**
RMSE	CASE A	2.50	2.29	2.38
	CASE B	2.60	2.46	2.44
	CASE C	2.70	1.92	**1.97**
	CASE D	2.53	1.99	**1.97**
	Fdda W	**2.22**	**1.73**	2.89
	Fdda L	2.24	1.74	2.89
MB	CASE A	-1.85	0.71	0.01
	CASE B	-1.78	0.71	0.36
	CASE C	-1.70	0.30	-0.09
	CASE D	-1.47	0.37	0.06
	Fdda W	-1.51	0.15	-1.74
	Fdda L	-1.50	0.18	-1.74
FB	CASE A	-0.007	0.003	0.000
	CASE B	-0.006	0.003	0.001
	CASE C	-0.006	0.001	0.000
	CASE D	-0.005	0.001	0.000
	Fdda W	-0.005	0.001	-0.006
	Fdda L	-0.005	0.001	-0.006

Solar Radiation (w/m^2)

Statistic	CASE	A1	A10	KR-R
R	CASE A	**0.85**	**0.91**	0.86
	CASE B	0.83	0.76	0.84
	CASE C	0.83	0.78	0.85
	CASE D	0.84	0.81	0.83
	Fdda W	0.76	0.89	**0.89**
	Fdda L	0.72	0.88	0.87
RMSE	CASE A	148.2	**122.4**	152.9
	CASE B	**148.0**	172.3	**144.5**
	CASE C	161.7	168.6	153.3
	CASE D	153.7	159.82	158.4
	Fdda W	192.9	146.07	164.08
	Fdda L	206.1	151.40	171.7
MB	CASE A	-32.3	-41.31	-52.02
	CASE B	-12.1	-3.28	-26.13
	CASE C	-30.9	-7.80	-41.12
	CASE D	-21.4	-8.31	-40.39
	Fdda W	-49.01	-54.18	-79.37
	Fdda L	-48.55	-53.43	-78.65
FB	CASE A	-0.183	-0.221	-0.300
	CASE B	-0.073	-0.020	-0.163
	CASE C	-0.170	-0.045	-0.242
	CASE D	-0.121	-0.048	-0.238
	Fdda W	-0.265	-0.280	-0.424
	Fdda L	-0.263	-0.277	-0.421

Wind speed (m/s)

Statistic	CASE	A1	A10	KR-R
R	CASE A	0.45	-0.21	**0.78**
	CASE B	**0.52**	-0.19	0.59
	CASE C	0.12	0.11	0.54
	CASE D	0.12	**0.22**	0.45
	Fdda W	0.33	-0.12	0.74
	Fdda L	0.33	-0.13	0.74
RMSE	CASE A	1.78	2.31	1.56
	CASE B	1.68	2.46	1.39
	CASE C	1.42	1.14	**0.60**
	CASE D	1.43	1.07	0.69
	Fdda W	1.42	**1.05**	0.98
	Fdda L	**1.41**	1.06	0.99
MB	CASE A	0.05	-1.27	-0.74
	CASE B	0.26	-1.22	-0.42
	CASE C	0.66	-0.58	0.11
	CASE D	0.83	-0.55	0.09
	Fdda W	-0.002	-0.38	-0.13
	Fdda L	-0.01	-0.39	-0.13
FB	CASE A	0.025	-0.795	-0.477
	CASE B	0.126	-0.779	-0.303
	CASE C	0.395	-0.454	0.117
	CASE D	0.531	-0.436	0.096
	Fdda W	-0.001	-0.335	-0.103
	Fdda L	-0.004	-0.338	-0.105

References

AJJAJI R., Ahmad A. AL-K., Khaled AL-C. 2008. Evaluation of United Arab Emirates WRF two-way nested model on a set of thick coastal fog situations, 2008 WRF workshop abstract.

Akylas, E., Kotroni, V., Lagouvardos, K., 2007. Sensitivity of high-resolution operational weather forecast to choice of the planetary boundary layer scheme. Atmospheric Research 84, 49–57.

Chen, S.-H., Sun, W.-Y., 2002. A one-dimensional ime dependent cloud model. Journal of the Meteorological Society of Japan 80, 99-118.

Grell, G.A., Dudhia, J., Stauffer, D.R., 1994. A Description of the Fifthgeneration Penn State/NCAR Mesoscale Model, *NCAR Technical Note* NCAR/TN-398 þ STR, 122 pp.

Hanna, S.R., 1994. Mesoscale meteorological model evaluation techniques with emphasis on needs of air quality models. In: Pielke, R.A., Pearce R.P. (Eds.), Mesoscale Modeling of the Atmosphere. Meteorological Monographs, Vol, 25. American Meteorological Society, Boston, MA 02108, 47-58.

Hong, S.-Y., Lim, J.-O., 2006. The WRF Single-Moment 6-Class Microphysics Scheme (WSM6). Journal of the Korean Meteorological Society 42, 129–151.

Hong, S.-Y., Noh, Y., Dudhia, J., 2006. A new vertical diffusion package with an explicit treatment of entrainment processes. Monthly Weather Review 134, 2318–2341.

Jose Rutllant, Rene Garreaud, 1994. Meteorological Air Pollution Potential for SANTIAGO, CHILE : Towards an Objective Episode Forecasting, *Environmental Monitoring and Assessment*, Vol, 34, 223-244.

Jeong J-H, Kim Y-K, 2009. The Application of High-resolution Land Cover and Its Effects on Near-surface Meteorological Fields in Two Different Coastal Areas, Journal of Korean Society for Atmospheric Environment, Vol. 25 (5), 432-449.

Kim jea-chul, 2010. Evaluation and Prediction of High Resolution Climate Simulation by Land Surface data Improve over Complex Terrain, Kangwon National University, PhD Thesis.

Lin, Y.L., Farley, R.D., Orville, 1983. Bulk water parameterization in a cloud model. J. Climate Appl. Met. 22, 1065-1092.

Olerud, D., Wheeler, N., 1997. Investigation of the Regional Atmospheric Modeling System (RAMS) for the Ozone Transport Assessment Group. Report to the Southeast Modelign Center, MCNC Environmental Programs, Research Triangle Park, NC 27709.

Song E. Y. 2007. Characterization of Observed High Ozone Phenomena over Seoul Metropolitan Area and Its Simulation with a Photochemical Model, Kangwon National University, PhD Thesis.

Zhao, P, Lüers, J, Olesch, J, Foken, T, 2011. Complex TERRain and ECOlogical Heterogeneity (TERRECO);WP 1-02: Spatial assessment of atmosphere-ecosystem exchanges via micrometeorological measurements, footprint modeling and mesoscale simulations ; Documentation of the Observation Period May 12th to Nov. 8th, 2010, Haean, South Korea, work report.

Whiteman C. D, Pospichal B., Eisenbach S., Weihs p., Clements C. B., Steinacker R., Erich M-R., Dorninger M., 2004. Inversion Breakup in Small Rocky Mountain and Alpine Basins, Journal of Applied Meteorology, Vol. 43, 1069-1082.